Preparation of Polymer Composites using Nanostructured Carbon Produced at Large Scale by Catalytic Decomposition of Methane

I. Suelves[a*], R. Utrilla, D. Torres, S. de Llobet, J.L. Pinilla, M.J. Lázaro, R.Moliner

[a] Instituto de Carboquímica, CSIC. Miguel Luesma 4, 50018 Zaragoza, Spain

Abstract

Polymer-based composites have been prepared using different concentrations of nanostructured carbons (NCs), produced by catalytic decomposition of methane (CDM). Four carbonaceous nanostructures were produced using different catalysts (with Ni and Fe as active phases), in a rotary bed reactor capable of producing up to 20 g of carbon per hour. The effect of nanostructured carbon on the thermal and electrical behaviour of epoxy-based composites is studied. An increase in the thermal stability and the decrease of electrical resistivity were observed for the composites at carbon contents as low as 1 wt%. The highest reduction of the electrical resistivity was obtained using multi-walled carbon nanotubes (MWCNTs) obtained with the Fe based catalysts. This effect could be related with the high degree of structural order of these materials. The results were compared with those obtained using a commercial carbon nanofibre, showing that the use of carbon nanostructures from CDM can be a valid alternative to the commercial nanofibres.

---

[*] Corresponding author: fax: +34 976 73 3318, e-mail address: isuelves@icb.csic.es

Key words: Polymer Matrix Composites; Nanostructured carbon; Electrical Properties;;

Catalytic Decomposition of Methane

1. Introduction

The catalytic decomposition of methane (CDM) is being studied for the simultaneous co-production of CO_2-free hydrogen and carbonaceous nanostructures. The catalysts traditionally used in CDM consist of transition metals belonging to groups 8 - 10 (such as Ni, Fe and Co) supported over different metal oxides (such as Al_2O_3 and MgO) [1]. These catalysts promote the formation of nanostructured carbon (NC) materials such as carbon nanofibres (CNFs) or carbon nanotubes (CNTs) with textural and structural properties that vary as a function of the catalyst composition and the operational conditions [2, 3]. These carbon materials and their possible applications play a key role in the economic feasibility of hydrogen production by CDM.

The packed bed reactor (PBR) and the fluidized bed reactor (FBR) are commonly used to perform CDM at a laboratory scale. The main drawback regarding PBR is the fact that the produced carbon is accumulated on the bed, which eventually causes reactor blockage [4-6]. This blockage can be avoided by working with an FBR because the catalyst and carbon mixture is continuously fluidized, increasing the height of the bed as the reaction proceeds. A third type of reactor configuration, a rotary bed reactor (RBR), has been suggested for the large-scale production of hydrogen and carbon nanofibres by CDM. Pirard et al. [7, 8] have used an inclined mobile-bed rotating reactor with rather slow carbon synthesis kinetics. They concluded that it is one of the most appropriate technologies for large-scale nanostructured carbon production. Our research group has compared the results obtained using nickel- and iron-based catalysts [9, 10] in an RBR and in an FBR under the same operating conditions. Tests conducted in the RBR showed higher hydrogen yields and more sustainable catalyst performance along with a more homogenous carbonaceous material compared to those obtained in the FBR.

Carbon produced by CDM has additional benefits due to its microstructure. For example, the morphology and textural (mainly mesopores-like) characteristics of CNFs or CNTs provide different potential applications, such as double layer capacitors,

electrocatalysts, carbon nanofibre-based composites or precursors of graphitic materials to be used as anodes within Li-ion batteries [11-14].

As regarding the preparation of composites, some authors [15] have shown how different types of CNFs can be used to reduce the electrical resistivity of the neat materials by several orders of magnitude; this effect has also been reviewed in [16]. Resistivities below 0.15 Ω·cm with a fibre loading near 15 wt% and a percolation threshold below 1 wt% have been reported [17]. The properties of nanocomposite materials are influenced by several factors like the size of its components and the degree of mixing between them. Therefore, the nature of the components and the method used to prepare them greatly influence the final properties. It is well known that epoxy resins are used as thermosetting matrices for manufacturing composites, since they provide good stiffness, specific strength, chemical resistance and good adhesion to the filler [18-24], making them suitable for applications in the electronic and aeronautic industries.

In a preliminary work, CNFs prepared using a Ni:Cu:Al catalyst in an FBR were tested as additives of epoxy resins, and the new material showed large decreases in electrical resistivity [21]. This study aims to investigate the influence of the structural and morphological properties of different as-produced nanostructured carbons on the electrical and thermal properties of epoxy-based composites. The NCs (CNFs and MWCNTs) were prepared by CDM in a rotary bed facility that allows hundreds of grams of very homogeneous materials to be produced every day. These materials were produced using four different catalysts under optimised experimental conditions, according to our previous results [2, 10, 21], and the effects caused by the as-prepared carbon material on the electrical and thermal properties of the composite were evaluated. The composites were compared with those obtained using commercial CNFs to assess the feasibility of using the NCs produced by CDM for this application.

2. Experimental

2.1 Materials

Carbon nanofilaments were prepared by CDM using four catalysts. Two of the catalysts selected for this study were Ni-based catalysts widely used in previous works [2, 21]: one used alumina as the textural promoter (denoted as $Ni:Al_2O_3$), and the other was nickel doped with copper over magnesia (denoted as Ni:Cu:MgO). The other two catalysts were iron over alumina (denoted as $Fe:Al_2O_3$) and iron doped with molybdenum and magnesia (denoted as Fe:Mo:MgO). The catalysts were prepared by the fusion method, which was described elsewhere [25]. To summarise, the respective nitric salts of the metals were mixed to form a powder that was subsequently heated at 350 °C for 1 h to promote the formation of the oxides, and the powders were calcined at 450 ºC for 8 h. The composition of each catalyst, expressed as the molar content of the reduced active phase and the textural promoter, was 80:20 ($Ni:Al_2O_3$), 78:6:16 (Ni:Cu:MgO), 67:33 ($Fe:Al_2O_3$) and 67:3:30 (Fe:Mo:MgO).

The CDM experiments were conducted in a rotary reactor installation that consists of a cylindrical drum made of Kanthal rotating around its horizontal axis. The diameter and length of the cylinder are 0.065 and 0.80 m, respectively, and the rotation speed can be varied from 1 to 20 rpm. More details of the experimental apparatus can be found in [9]. Prior to the reaction, the catalysts were reduced in a hydrogen atmosphere. The CDM reaction temperature was established at 700 ºC for the Ni-based catalysts and 800 ºC for the Fe-based ones. Ten grams of each catalyst were used for each run. Pure methane was fed for 3 h adjusted to a weight hourly space velocity (WHSV, defined here as the methane flow rate at normal conditions per gram of catalyst initially loaded) of 12 Nl $CH_4 \cdot (h \cdot g_{cat})^{-1}$. Additionally, a commercial CNF (PR-24-XT-LHT, produced by Applied Sciences, Inc.) has also been used for comparison. According to the manufacturer, the sample is produced in a floating catalyst system with iron pentacarbonyl using natural gas, H_2S, air and NH_3. The fibres are debulked and thermally treated at a temperature of

5

1500 ºC to provide the best compounding properties and the highest electrical conductivity in the nanocomposites.

2.2 Characterisation of the NCs

X-ray diffraction (XRD) analysis of the carbon nanostructures was performed in a Bruker D8 Advance Series 2 diffractometer using a Bragg-Brentano θ-θ configuration, Ni –filtered Cu Kα radiation and a secondary graphite monochromator. The angle range scanned was 3–80º, with a step size of 0.05º and a scan step of 3s.

The textural properties of the carbon nanostructures were measured by N_2 adsorption at 77 K in a Micromeritics ASAP 2020 apparatus. The specific surface area and pore volume were calculated by applying the BET method.

Electrical conductivity measurements were performed while applying pressures from 0.5 to 80 MPa on the powder NCs using a manual hydraulic press. The electrical resistance was measured by applying electrical currents up to 0.015 A. The height of the cylinder in which the powder is introduced and pressed was determined with a digital Mitutoyo micrometer with an accuracy of ± 0.02 mm.

Transmission electron microscopy (TEM) was performed using a Jeol 2011 microscope equipped with an LaB_6 gun operating at 200 kV on the carbon sample obtained with the $Ni:Al_2O_3$ catalyst and the commercial CNF, whereas a Jeol-2000 FXII microscope was used for those obtained with the Ni:Cu:MgO, $Fe:Al_2O_3$ and Fe:Mo:MgO catalysts. The samples were first finely ground and dispersed in ethanol. A drop of this solution was then deposited on a standard TEM copper grid previously coated with a lacy amorphous carbon film.

2.3 Preparation and characterisation of the nanocomposites

A commercial epoxy resin named Triepox LM (supplied by GAIRESA) was used as the polymer matrix. This resin is based on a highly functionalised epoxy resin with non-modified cycloaliphatic amines. Triepox LM is polymerised by a hardener with the same name in a ratio of 2,35/1 by weight (matrix/hardener). The final product has a low viscosity of 200 mPa according to ASTM D2393-86.

To prepare the composites, 0.5 to 14 wt% of as-grown carbonaceous material was dispersed in the resin. First, the carbonaceous material and the epoxy were mixed by a 100 W ultrasonic bath for 30 minutes at room temperature. Then, the hardener was added to the mixture, which was sonicated at room temperature for an additional 15 minutes. The composites were cured for 24 h at room temperature and post-cured for 5 h at 70 ºC following the manufacturer's recommendations.

The specimens were processed into tablets that were 17 mm in diameter and 3 mm in thickness (e). Their electrical resistance (R) was averaged from the I-V curves measured at different applied voltages. To obtain a good electrical contact, both surfaces (each with an area of A) of the specimen were coated with a conductive silver paint. The electrical resistivity corresponds to the inverse of the electrical conductivity (ρ) of the composites, which is calculated according to equation (1):

$$\rho = \frac{R \cdot A}{e} \qquad (1)$$

Thermal gravimetric analysis (TGA) were conducted using a SETARAM analyser. 10 mg of the composites were placed in a platinum crucible and heated in air. The heating rate was 10 ºC/min up to 800 ºC under a constant air flow of 20 ml/min.

A Hitachi S-3400 scanning electron microscope was used to analyse the distribution of the NC within the polymer matrix. The specimens were covered by a layer of gold to make them electrically conductive.

3. Results and discussion

3.1 Characterisation of the NCs

As mentioned in an earlier section, the catalysts and operation parameters used to prepare the NCs were selected according to previous results obtained by our research group [2, 25]. A summary of NCs main properties can be found in [10] and in Table 1; some examples of typical TEM micrographs of the structure of these NCs are given in Fig 1. Also the properties of the commercial nanofibres used for comparison (section 3.2.3.2) are included in Table 1 and Fig 1. The four carbon materials are named as follows: those produced using the Ni:Al$_2$O$_3$ catalyst as NC1, the ones obtained using the Ni:Cu:MgO catalyst as NC2, those obtained with the Fe:Al$_2$O$_3$ catalyst as NC3 and NC4 refers to the materials prepared using Fe:Mo:MgO catalyst.

The specific surface area of these materials range from 37 to 76 m^2/g, mainly due to the presence of mesopores. The four carbon materials produced (labelled in the format "catalyst-NC"; e.g., "Ni:Al$_2$O$_3$-NC") show a significant degree of structural order corresponding to a turbostratic carbon structure. Of the two types of catalysts, the carbonaceous structures produced with Fe-based catalysts were more ordered compared to those produced with Ni-based catalysts, according to the value of the interlaying spacing d$_{002}$ and the crystal domain size Lc. The textural properties of the carbon materials are mainly mesoporous, with the pores located in the interior of the fibre and in the spaces between the filaments. The electrical conductivity of the four materials range from 21 S/cm for NC1 and NC2, to 30 S/cm for NC4 which is in complete agreement with the structural order data.

The four carbon materials were deposited mainly in the form of nanostructures with varying morphology (diameter and length) depending on the catalyst used. The diameter of the filaments correlates with the size of the catalyst particle. The effect of the presence of Mo and Cu, the use of different catalyst supports (Al$_2$O$_3$ or MgO) and also the reaction temperature on the size and shape of catalyst particles should be considered [2, 25]. Anyway, it is difficult to establish a general conclusion about the exact nature of

8

each material, because in a sample, different morphologies, diameters and lengths of CNs can be observed.

 Both NC1 (Fig 1a) and NC2 (Fig 1b) exhibit a fishbone structure characterised by the presence of sloping graphitic layers with respect to the longitudinal axis of the fibre. Although these two NCs have similar structures, some interesting differences related to the diameter of the nanofibres could be observed. The NC1 samples are quite homogeneous (Fig 1a), and they are approximately 50 nm in diameter. On the other hand, the NC2 samples showed two main sizes, as observed in Fig 1b. The larger nanofibers had diameters up to 400 nm, whereas the smaller ones did not exceed 25 nm. For the NCs obtained with the two Fe-based catalysts (Fig 1c-1d), multi-walled carbon nanotubes (MWCNTs) and chain-like CNFs were observed, as previously noted by other authors [3, 27]. NC3 shows the highest aspect ratio (length/diameter) and the absence of amorphous carbon while NC4 is formed by carbon nanofilaments with a higher heterogeneity in diameter and length [10]. Commercial CNFs were also analysed by TEM (Fig 1e-1f). Two different structures were observed, fishbone and chain-like CNFs. Due to the heat treatment at which commercial CNFs have been submitted (1500ºC), the walls have almost no defects and a great homogeneity is observed. These nanofibres present an average diameter of 100nm with huge hollow core which represents almost the entire width and no catalyst particles are noticed.

3.2 Characterisation of the epoxy composites

3.2.1 Microstructure

SEM analyses of the composites are shown in Fig 2-4. According to Fig 2a, the NCs are dispersed and form clusters or agglomerates along the sample (Figure 2a). In Figure 2b is shown an example of a cluster in which the fibres are dispersed in the epoxy matrix forming a network. However, these kinds of clusters cannot be observed in the composites filled with NC2 (Fig 3a) because the fibres are mainly isolated, as seen in

Fig 3b; nevertheless, some NCs with larger diameters are inserted into the matrix. Fig 4 shows the micrographs of the composites filled with different contents of NC4 (2, 8 and 14 wt% NC). In the low magnification micrographs (named with the suffix "l"), the NC4 are seen to agglomerate and form clusters within the resin.. The size of these clusters increases with the NC content in both cases, as seen in Fig 4a-l, 4b-l and 4c-l. These clusters are not so easily identified in NC3 (Figure not shown).

As mentioned in section 3.1 the NC1 sample consists of more homogeneous nanofilaments narrower than NC2. Regarding the nanofilaments obtained with the Fe-based catalysts, the NC3 show highest aspect ratio (length/diameter) and NC4 are nanofilaments with a higher heterogeneity in diameter and length In conclusion it seems that the different morphology, diameter and homogeneity (consequence of the different type of catalyst used to prepare them) could be responsible of the different dispersion behaviour observed.

In the high magnification micrographs (Fig 4, named with the suffix "h"), gaps and voids can also be observed. The existence of voids and pores is an undesired phenomenon that appears to be more frequent as the NC content increases what emphasises the need to improve the preparation process if high filler content is necessary.

3.2.2 Thermal properties

Fig 5a shows the TGA curves for the pure epoxy matrix, the NC1 sample and the composites with different NC1 contents plotted after substractiong the TGA data from the NC1 without the matrix. The epoxy resin starts to decompose at temperatures around 220 ºC while for the NC1 sample, the starting decomposition temperature is 490ºC. The composites prepared withNC1 decomposed at higher temperatures with increasing filler content and the effect was observed even at the starting temperature of decomposition . For example, 1% of the epoxy resin is decomposed at 224ºC while

10

more than 250ºC are needed to obseve the same weight loss for the 14%-NC1 composite. The epoxy resin is almost completely decomposed at 540ºC (95% weight lost) while 597º and 620ºC are needed for the 10%wt and 14%wt-NC1 composites respectively. Therefore, the incorporation of the NCs helps to stabilise the matrix and prevents decomposition. Similar effects have been reported in the past for composites prepared with epoxy resins and also other polymer based composites [20].

Regarding the composites prepared with NC3, shown in Figure 5b, a similar trend was observed, although the effect was not so important for the lowest content composites or at the starting temperature of decomposition. For the composites prepared with 10 and 14%wt and especially for temperatures above 400ºC the estabilization effect was noted. For example a 75% wt is obtained at 402ºC for the pure epoxy resin while 439º and 463ºC are needed for the two composites.

3.2.3 Electrical properties

3.2.3.1 Composites prepared using NCs from CDM

The electrical resistivity curves of the composites filled with the four NCs are shown in Fig 6. The value of the electrical resistivity of the neat resin lies beyond the detection limit of our measurement device, and it is estimated at approximately 10^{11} $\Omega \cdot$cm.

In the two series of composites filled with NC prepared with Ni-based catalysts, the electrical resistivity of those prepared with NC2 starts to decrease at a NC load of 4 wt%, reaching a value of 1.5×10^7 $\Omega \cdot$cm with 10 wt%. The electrical resistivity stopped decreasing at higher NC loads. For the composites prepared with NC1, the electrical resistivity (1.0×10^9 $\Omega \cdot$cm) begins decreasing at an NC content of 10 wt%; it continued to decrease as the NC content increased, reaching a value of 2.6×10^7 $\Omega \cdot$cm at approximately 14 wt%.

11

On the other hand, the electrical resistivity of the composites with NC3 and NC4 decreased considerably with very low amounts of filler. For instance, 1 wt% of NC4 is required to obtain a composite with an electrical resistivity of 2.88×10^5 Ω·cm, and 1 wt% of NC3 is needed to obtain an electrical resistivity of 1.5×10^6 Ω·cm. Once this minimum content of NC has been added, the electrical resistivity of the composites decreases progressively until a minimum of 94 Ω·cm for the NC4 sample (14 wt%). The percolation theory can be applied to explain the behaviour of these composites because their measured electrical resistivity sharply decreases by several orders of magnitude when a critical amount of filler has been added. The decrease is due to the formation of continuous electron paths, and the resistivity continues to decrease slowly with increasing NC content [16, 28].

It has been reported [29] that conventional conducting fillers need contents as high as 10 – 15 wt%, resulting in a composite with poor mechanical properties and high density. Lower nanofilament concentrations will allow better dispersion and higher mechanical performance in future applications [15, 17] and so, NCs obtained by CDM with Fe-based catalysts seem to be promising additives at low loadings.

According tho the data shown in Table 1, the NC´s used to prepare the composites have an important residual metal content, especially high for the composites prepared with NC3 and NC4. To reduce the metal content of the samples and discard its possible effect on the electrical properties, NC1 and NC4 were chemically treated with concentrated (65% wt) nitric acid (100 ml) at room temperature for two hours under 700 rpm. These two new types of NCs are named as NC1- HNO_3 and NC4-HNO_3. The metal content was reduced form 12.01 to 4.51 for the NC1 sample and from 30.60 to 11.9% (wt) for the NC4. New composites were prepared using the acid treated samples without significantly varying the rest of properties as shown in previous works [29, 30], and the results obtained for the electrical resistivity are presented in Figure 7 and

compared to those obtained for the non-treated samples. Very similar results were obtained and so, it is possible to establish that the good results obtained with CNF from Fe-based catalysts are not due to the high metal content.The large differences observed between the electrical resistivity of the composites filled with NC made from Ni-based and Fe-based catalysts can be explained by the morphologies and structures of those materials. The NCs produced with the Fe catalysts show a higher degree of structural order. In addition, these carbon materials had a mixture of chain-like NCs and MWNTs, as observed in Fig 1f - h.

3.2.3.2 Comparison of the electrical properties of the composites filled with CDM-NCs and commercial CNFs

In addition, Fig 6 shows the electrical resistivity of the composites filled with the commercial NC (named PR24-XT-LHT). For the composites prepared with low NC content (up to 2 wt%), the lowest electrical resistivity is obtained when the NCs made with the Fe catalysts are used as additives. The electrical resistivity of the composites filled with NC3 and NC4 at 1 wt% was 1.5×10^6 $\Omega \cdot$cm and 2.8×10^5 $\Omega \cdot$cm, respectively; whereas the resistivity of the composite filled with the PR24-XT-LHT at 1 wt% was 4.1×10^{10} $\Omega \cdot$cm. On the other hand, once the NC content is over 2 wt%, the best results are obtained with the PR24-XT-LHT nanofibre. In fact, more than double the percentage of NC4 (14 wt%) is necessary to obtain results similar to the results when PR-24-XT-LHT is used (6 wt%).

Considering that the goal of this work is to produce electrically conductive composites with the lowest possible filler concentration without diminishing the mechanical properties, the as-prepared NC from CDM using Fe-based catalysts may be an interesting alternative to commercial NCs when working at low NC content.

Additional work is in progress to improve the dispersion of NCs into the matrix by modifying the initial properties of the carbon material and also by optimizing the preparation process.

4. Conclusions

Nanostructured carbons obtained at a large scale have been used as additives to prepare epoxy-composites by CDM. Compared to pure resin, the thermal stability of these composites was enhanced; in addition, their electrical resistivity decreased even at low filler contents. The best results were observed for the nanostructured carbon prepared using Fe-based catalysts, mainly composed by chain like NCs and MWCNT and showing a higher degree of structural order as compared to those materials produced with Ni-based catalysts. The composites prepared using these carbon materials have similar properties to those prepared using commercial NCs.

5. Acknowledgements

6. References

[1] Abbas HF, Wan Daud WMA (2010) Hydrogen production by methane decomposition: A review. International Journal of Hydrogen Energy; 35: 1160–1190.

[2] Pinilla JL, Suelves I, Lázaro MJ, Moliner R, Palacios JM. (2009) Influence of nickel crystal domain size on the behaviour of Ni and NiCu catalysts for the methane decomposition reaction. Applied Catalysis A: General ; 363:199-207.

[3] Martin-Gullon I, Vera J, Conesa JA, González JL, Merino C (2006) Differences between carbon nanofibers produced using Fe and Ni catalysts in a floating catalyst reactor. Carbon; 44:1572-80.

[4] Muradov N (2001) Hydrogen via methane decomposition: An application for decarbonisation of fossil fuels. Int. Journal of Hydrogen Energy 2001; 26:1165-1175.

[5] Pinilla JL, Suelves I, Lázaro MJ, Moliner R, Palacios JM (2010) Parametric study of the decomposition of methane using a $NiCu/Al_2O_3$ catalyst in a fluidized bed reactor. International Journal of Hydrogen Energy ; 35 (18): 9801-9809

[6] Pinilla JL, Lázaro MJ, Suelves I, Moliner R, Palacios JM. (2010) Characterization of nanofibrous carbon produced at pilot-scale in a fluidized bed reactor by methane decomposition. Chemical Engineering Journal; 156: 170-76.

[7] Pirard SL , Pirard JP, Bossuot C. (2009) Modeling of a continuous rotary reactor for carbon ianotube synthesis by catalytic chemical vapor deposition. AIChE J.; 55: 675–686.

[8] Pirard SL, Lumay G, Vandewalle N, Pirard JP (2009) Motion of carbon nanotubes in a rotating drum: The dynamic angle of repose and a bed behavior diagram. Chem. Eng. J. ; 146:143–147.

[9] Pinilla JL, Utrilla R, Lázaro MJ, Suelves I., Moliner R, Palacios JM. (2009) A novel rotary reactor configuration for simultaneous production of hydrogen and carbon nanofibers. International Journal of Hydrogen Energy ; 34: 8016-22.

[10] Pinilla JL, Utrilla R, Lázaro MJ, Moliner R, Suelves I, García AB (2011) Ni and Fe –based catalysts for hydrogen and carbon nanofilament production by catalytic decomposition of methane in a rotary bed reactor. Fuel Processing Technology; 92:1480-1488.

[11] Tao XY, Zhang XB, Zhang L, Cheng JP, Liu F, Luo J, et al.(2006) Synthesis of multi-branched porous carbon nanofibers and their application in electrochemical double-layer capacitors. Carbon;44:1425-28.

[12] Zheng JS, Zhang XS, Li P, Zhu J, Zhou XG, Yuan WK. (2007) Effect of carbon nanofiber microstructure on oxygen reduction activity of supported palladium electrocatalyst. Electrochemistry Communications ;9: 895-900

[13] Maruyama B, Alam K. (2002) Carbon nanotubes and nanofibers in composite materials. SAMPE Journal;38:59-70.

[14] Yoon SH, Park CW, Yang H, Korai Y, Mochida I, Baker RTK, et al. (2004) Novel carbon nanofibers of high graphitization as anodic materials for lithium ion secondary batteries. Carbon ;42:21-32.

[15] Vera-Angulo J, Glória-Pereira A, Valera-Rizo H., González JL, Martin-Gullón I., (2009) Comparative study of the dispersion and functional properties of multiwall carbon nanotubes and helical-ribbon carbon nanofibres in polyester nanocomposites. Composites Science and Technology ; 69:1521-1532

[16] Al-Saleh MH, Sundararaj U. (2009) A review of vapour grown carbon nanofiber/polymer conductive composites. Carbon ;47: 2-22.

[17] Tibbets GG, Lake ML, Strong KL, Rice BP. (2007) A review of the fabrication and properties of vapour-grown carbon nanofiber/polymer composites. Composites Science and Technology ; 67:1709-1718.

[18] Hammel E, Tang X, Trampert M, Schmitt T, Mauthner K, Eder A, Pötschke P, (2004) Carbon nanofibers for composite applications. Carbon ; 42:1153-1158.

[19] Zhamu A, Hou Y, Zhong W-H., Stone JJ, Li J, Lukehart CM. (2007) Properties of a reactive graphitic carbon nanofibers reinforced epoxy. Polym. Compos. ; 605-611.

[20] Choi YK, Sugimoto K, Song SM, Gotoh Y, Ohkoshi Y, Endo M. (2005) Mechanical and physical properties of epoxy composites reinforced by vapour grown carbon nanofibers. Carbon ;43:2199-2208.

[21] Utrilla R, Pinilla JL, Suelves I, Lázaro MJ, Moliner R. (2011) Catalytic decomposition of methane for the simultaneous co-production of CO_2-free hydrogen and carbon nanofibre based polymers. Fuel;90:430-432.

16

[22] Cardoso P, Silva J, Paleo AJ, J. van Hattum FW, Simoes R, Lanceros-Mémdez S. (2010) The dominat role of tunneling in the conductivity of carbon nanofiber-epoxy composites. Phys. Status Solidi A ; 207:407-410.

[23] Sandler J, Shaffer MSP, Prasse T, Bauhofer W, Schulte K, Windle AH, (1999) Development of a dispersion process for carbon nanotubes in an epoxy matrix and the resulting electrical properties. Polymer ; 40:5976-5971.

[24] Bal S. (2010) Experimental study of mechanical and electrical properties of carbon nanofiber/epoxy composites. Materials and Design ;31:2406–2413.

[25] Pinilla JL, Utrilla R, Karn RK, Suelves I, Lázaro MJ, Moliner R, García AB, Rouzaud JN. (2011) High temperature iron-based catalysts for hydrogen and nanostructured carbon production by methane decomposition. Int. J. Hyd. Energy 36: 7832-7843.

[26] Suelves I., Lázaro MJ, Moliner R, Echegoyen Y, Palacios JM. (2006) Ni and Ni–Cu catalysts development for hydrogen production by catalytic decomposition of methane. Catalysis Today ; 116:271–80.

[27] Ermakova MA, Ermakov DY, Chuvilin AL, Kuvshinov GG.(2001) Decomposition of Methane over Iron Catalysts at the Range of Moderate Temperatures: The Influence of Structure of the Catalytic Systems and the Reaction Conditions on the Yield of Carbon and Morphology of Carbon. Journal of Catalysis ; 201:183-197.

[28] Ma P-C, Siddiqui NA, Marom G, Kim J-K. (2010) Dispersion and functionalization of carbon nanotubes for polymer based nanocomposites: A review. Composites: Part A:1345-1367.

[29] Calvillo L., Lázaro MJ, Suelves I, Echegoyen Y, Bordejé EG, Moliner R. (2009) Study of the surface chemistry of modified carbon nanofibers by oxidation treatments in liquid phase. Journal of Nanoscience and Nanotechnology; 9 (7): 4164-4169

[30] Sebastián D, Suelves I, Moliner R, Lázaro MJ. (2010). The effect of the functionalization of carbon nanofibers on their electronic conductivity. Carbon 48; (15) : 4421-4431

FIGURE CAPTIONS

Fig 1. TEM micrographs of the NC obtained by CDM with (a) NC1, (b) NC2, (c) NC3, (d) NC4 and of the commercial PR-24-XT-LHT (e)-(f).

Fig 2. SEM micrographs of the composites filled with 14 wt% NC1. Low (l) and high magnification (h);

Fig 3. SEM micrographs of the composites filled with 14 wt% NC2. Low (l) and high magnification (h).

Fig 4. SEM micrographs of the composites filled with 2 (A), 8 (B) and 14 wt% (C) NC4. Low (l) and high magnification (h).

Fig 5. TGA curves of pure epoxy resin, NC and composites at various loadings. (a) NC1 composites; (b) NC3 composites

Fig 6. Electrical conductivity of the composites filled with both CDM-NC and commercial NC.

1   **Table 1.** BET surface area (S_{BET}), interlaying spacing (d_{002}), crystal domain size (Lc)

2   and metal content (%) of the nanostructured carbon.

Sample	Catalyst used	S_{BET} (m^2/g)	d_{002} (nm)	Lc (nm)	Metal content (%)
NC1	Ni:Al$_2$O$_3$	76	0.3420	5.7	12.0
NC1-HNO3	Ni:Al$_2$O$_3$	83	0.3390	5.9	4.5
NC2	Ni:Cu:MgO	72	0.3386	8.4	7.3
NC3	Fe:Al$_2$O$_3$	65	0.3382	10.3	36.2
NC4	Fe:Mo: MgO	89	0.3356	11.3	30.7
NC4-HNO$_3$	Fe:Mo: MgO	104	0.3365	11.0	11.9
PR-24-XT-LHT	Iron based	37	0.3382	5.4	4.7

3

4

5

6

1   **Figure 1**
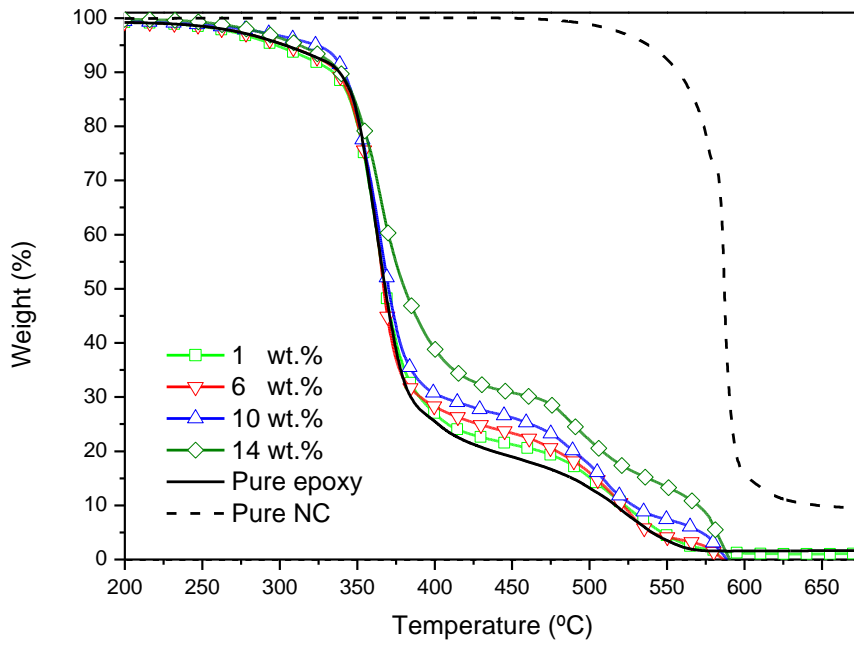
2
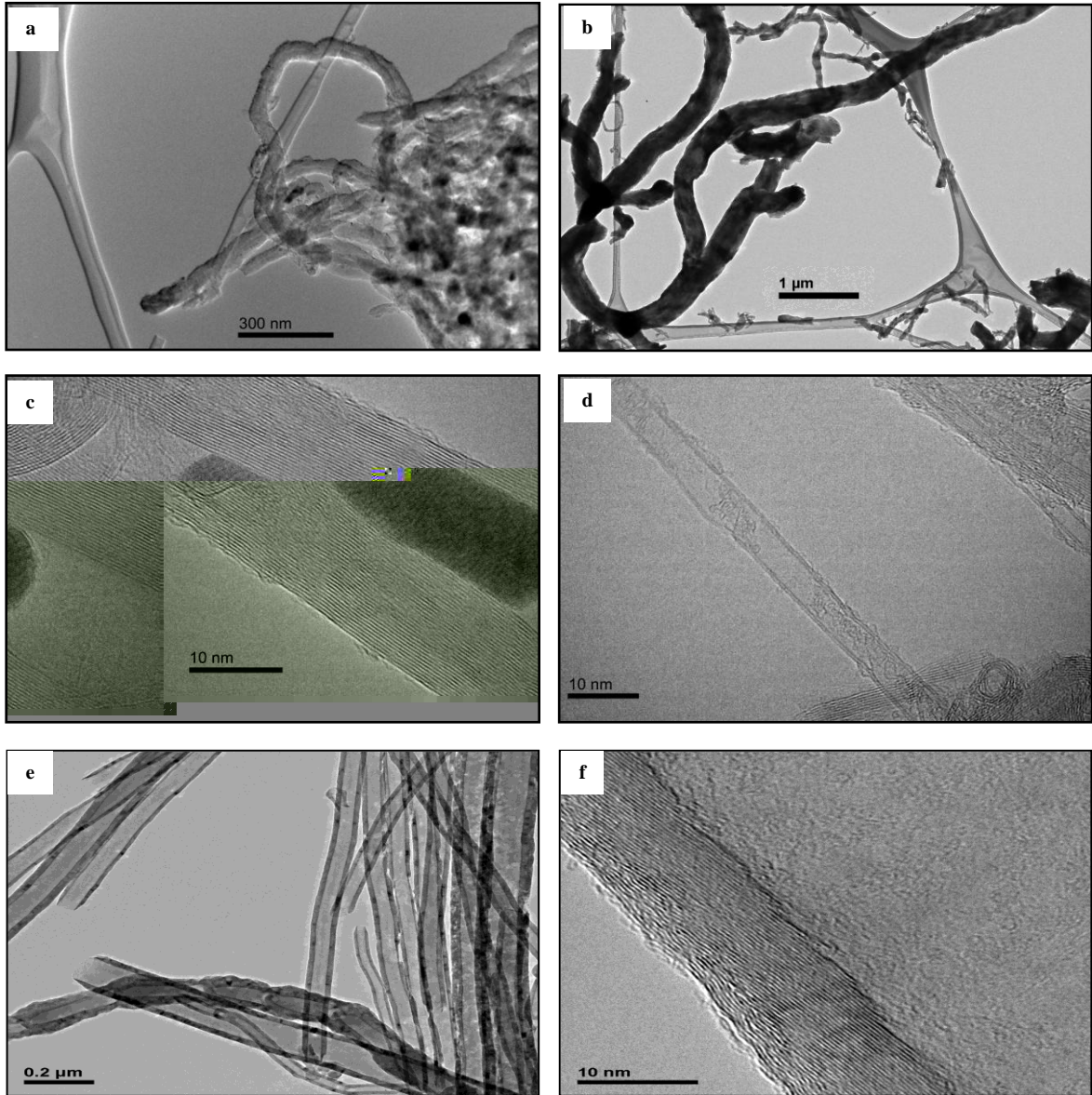
Figure 2
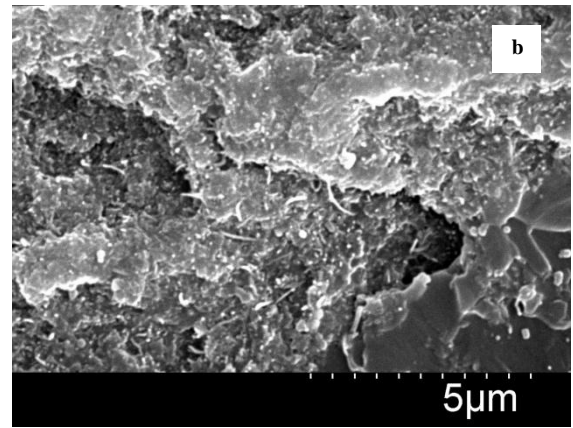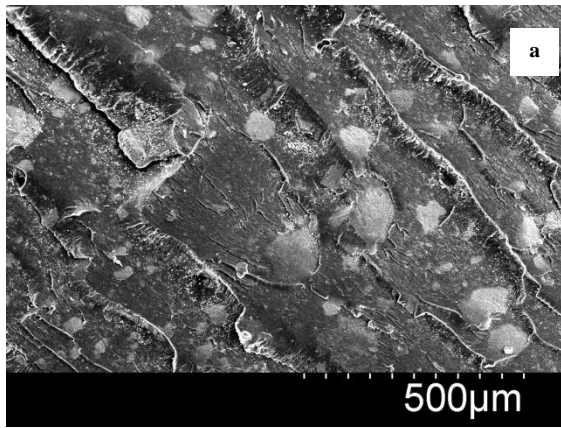
Figure 3
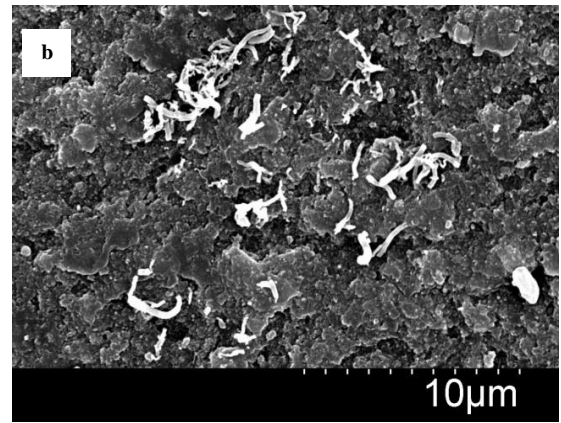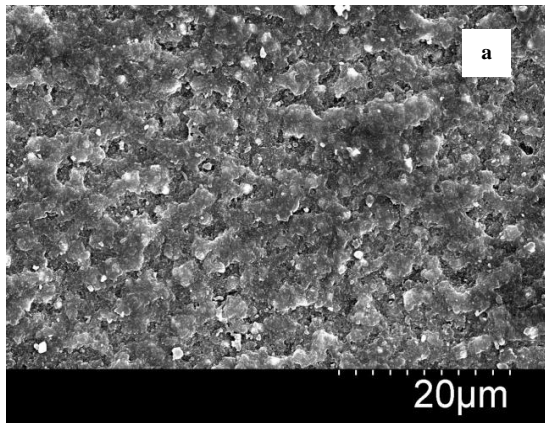
Figure 4
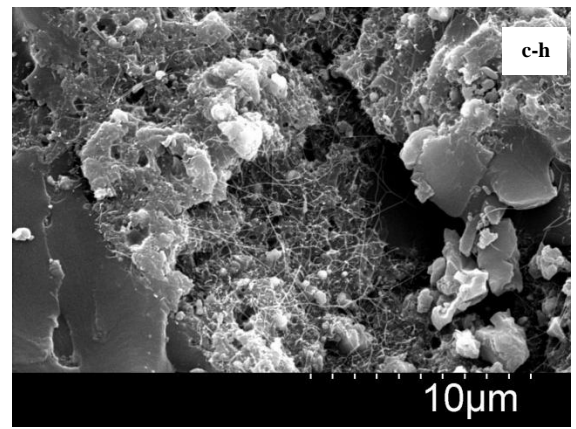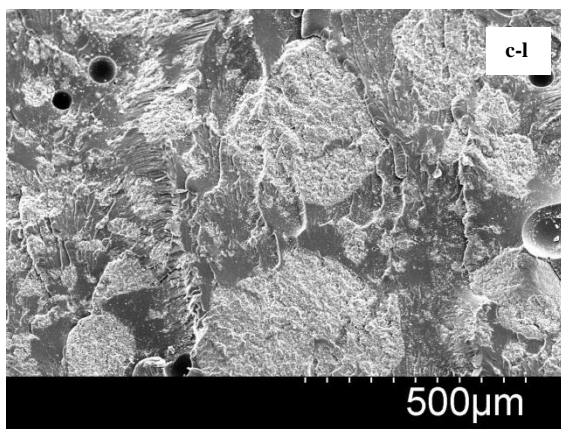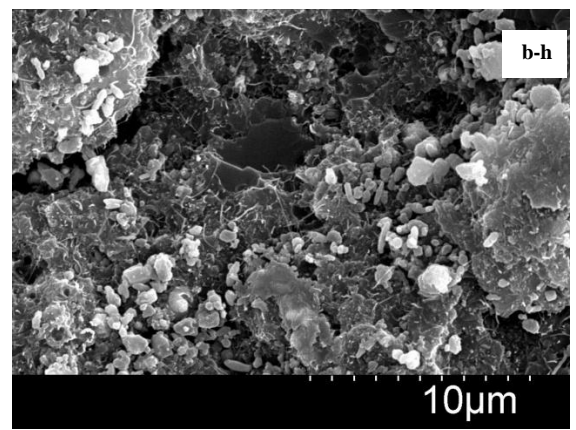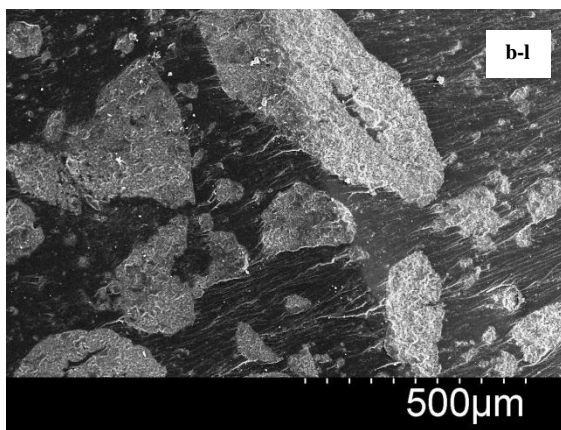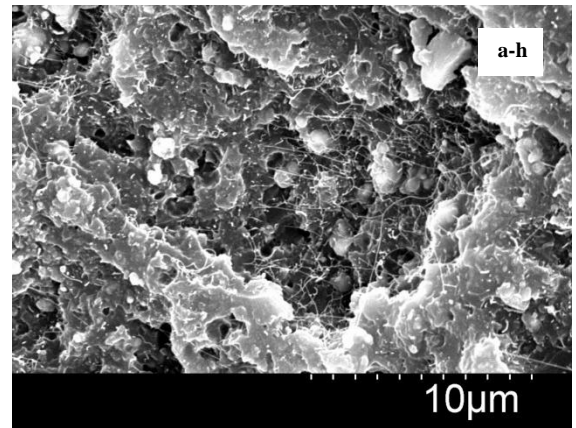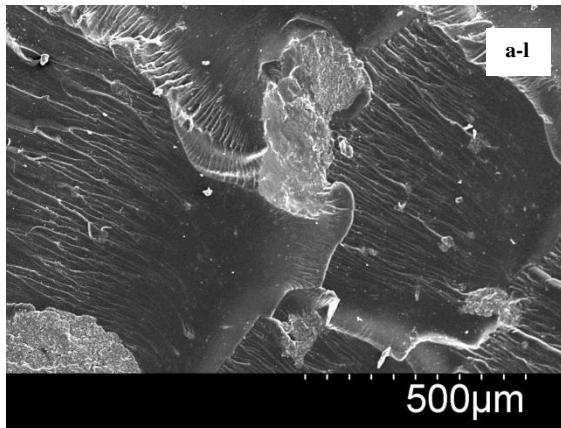
1   **Figure 5**

2   **a)**

3

4   b)

1   **Figure 6**

2

1 **Figure 7**

2